

Kinematics of iterative interferometry in a passive seismic experiment

Sjoerd de Ridder*, George Papanicolaou and Biondo Biondi, Stanford University.

SUMMARY

We study a novel approach to seismic interferometry; iterative interferometry. To utilize secondary Huygens sources that illuminate the medium from regions where primary sources are absent, we correlate the coda of correlations. We identify the leading terms in the second round of correlations and study their kinematics using correlation gathers. We discuss how iterative interferometry can improve the Green's function estimation with respect to conventional interferometry.

INTRODUCTION

It has long been known that correlations of ambient seismic noise recorded at two stations can yield the Green's function between the two stations (Aki, 1957; Claerbout, 1968; Lobkis and Weaver, 2001; Wapenaar, 2004). For an overview of the theory of seismic interferometry (SI) and its applications we refer to the SEG reprint series Wapenaar et al. (2008a). The conditions for Green's function retrieval by SI can be described as energy equipartitioning in the ambient seismic field; i.e. the energy current is equal in all directions. Breakdown of this requirement leads to imperfect Green's function reconstruction (Malcolm et al., 2004; Paul et al., 2005; Artman, 2007; Miyazawa et al., 2008).

Stehly et al. (2008) propose a novel procedure to improve the estimated Green's functions (EGFs); by correlating the coda of correlations of ambient seismic noise, C^3 . They reason that the coda of an EGF contains information from secondary scattering in the medium, analogous to Green's function estimation by coda wave interferometry (Snieder, 2004; Malcolm et al., 2004; Paul et al., 2005; de Ridder and Prieto, 2008). Garnier and Papanicolaou (2009) prove the validity of this procedure based upon stationary phase analysis of the leading terms in the iterated correlation.

We study an example with two main stations surrounded by a network of auxiliary stations, in the presence of an additional scatterer positioned at the stationary phase region of the GF between the two main stations. We analyze the kinematics of the events in C^3 for sensitivity to auxiliary receiver location and source location. This study has implications for seismic exploration using ambient seismic noise for different acquisition geometries, as in a network of stations on the surface recording the ambient field above a reservoir, or a borehole survey with stations down-hole and on the surface.

CONVENTIONAL INTERFEROMETRY VERSUS ITERATIVE INTERFEROMETRY

Conventional SI aims to retrieve the Green's function between two stations by correlating records of an ambient field, in which

the energy is equipartitioned. It is generally assumed that energy equipartitioning should be obtained after averaging over sources that excite the background field (Snieder et al., 2007).

Sources located at stationary phases are necessary to retrieve good quality EGFs. An example are sources I in Figure 1(a) are located on a ray path from receiver B extending to and beyond receiver A. Correlating responses from these sources recorded at A and B will retrieve a good quality GF. However sources II in Figure 1(a) are not located in the stationary phase region, correlating responses from these sources recorded at A and B will retrieve a poor quality GF. Various authors have

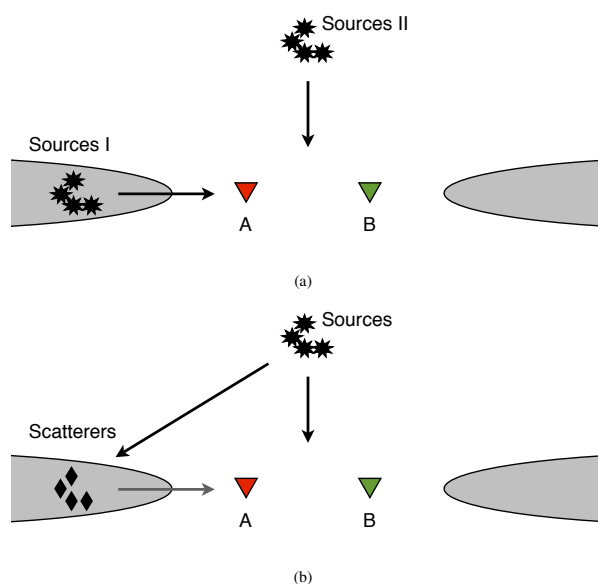


Figure 1: (a) Source positions I and II for respectively good and poor quality Green's function estimation by conventional SI, stationary phase regions are indicated by gray areas. (b) Source and scatterer positions for improved Green's function estimation by iterative SI.

proposed methods to compensate for anisotropic illuminations; beam forming and weighting the data for different directionality components (Stork and Cole, 2007), multidimensional deconvolution after the identification of individual responses (Wapenaar et al., 2008b). Stehly et al. (2008) propose a novel procedure to improve the estimated Green's functions (EGFs) by utilizing the secondary Huygens' sources of scatterers positioned at the stationary phase positions. Their utilization is proposed in three steps (Stehly et al., 2008); First, the recordings at two main stations are correlated with a network of auxiliary stations. Each correlation yields an EGF. Second, each EGF is muted for times prior to an estimated arrival time. Third, a correlation, C^3 , is evaluated between the muted EGF pairs estimated for each auxiliary station. Which is subsequently averaged across the network of auxiliary stations.

THEORY OF ITERATIVE INTERFEROMETRY

First we study the leading terms in the correlation of muted EGFs. The Green's function of a source at \mathbf{x}_s in a medium containing one scatterer at \mathbf{x}_c under the Born approximation contains two terms:

$$G(\mathbf{x}, \mathbf{x}_s, \omega) = G_0(\mathbf{x}, \mathbf{x}_s, \omega) + G_1(\mathbf{x}, \mathbf{x}_s, \omega), \quad (1)$$

$$G_1(\mathbf{x}, \mathbf{x}_s, \omega) = \frac{\omega^2}{c^2} G_0(\mathbf{x}, \mathbf{x}_c, \omega) G_0(\mathbf{x}_c, \mathbf{x}_s, \omega) \alpha. \quad (2)$$

The correlation function, $C_{i,j}^2$ (superscript refers to the number of station recordings combined through correlation), is constructed between the recording made at stations at \mathbf{x}_i and \mathbf{x}_j as

$$\begin{aligned} C_{i,j}^2(\omega) &= G(\mathbf{x}_i, \mathbf{x}_s, \omega) G^*(\mathbf{x}_j, \mathbf{x}_s, \omega) = \\ &G_0(\mathbf{x}_i, \mathbf{x}_s, \omega) G_0^*(\mathbf{x}_j, \mathbf{x}_s, \omega) + G_0(\mathbf{x}_i, \mathbf{x}_s, \omega) G_1^*(\mathbf{x}_j, \mathbf{x}_s, \omega) + \\ &G_1(\mathbf{x}_i, \mathbf{x}_s, \omega) G_0^*(\mathbf{x}_j, \mathbf{x}_s, \omega) + G_1(\mathbf{x}_i, \mathbf{x}_s, \omega) G_1^*(\mathbf{x}_j, \mathbf{x}_s, \omega), \end{aligned} \quad (3)$$

where the 4 terms on the right hand side will be referred to as terms 3.1, 3.2, 3.3, and 3.4, respectively. Term 3.1 is the leading term, terms 3.2 and 3.3 are of order α , term 3.4 is of order α^2 . The first round of correlations computes $C_{A,X}^2(t)$ and $C_{B,X}^2(t)$. The retrieved signals are muted in the time domain to exclude term 3.1, yielding $\tilde{C}_{A,X}^2(t)$ and $\tilde{C}_{B,X}^2(t)$. Now a second correlation function is evaluated correlating $\tilde{C}_{A,X}^2(\omega)$ and $\tilde{C}_{B,X}^2(\omega)$ and averaging over a network of A auxiliary stations,

$$\tilde{C}_{B,A}^3(\omega) = \frac{2c}{i\omega} \sum_{a=1}^A \tilde{C}_{B,X}^2(\omega) \left\{ \tilde{C}_{A,X}^2(\omega) \right\}^*. \quad (4)$$

The proportionality factor is chosen such that the $\frac{\omega^2}{c^2}$ factor in equation 2 is matched to the proportionality factor $\frac{-2i\omega}{c}$ appearing in the exact interferometric Green's function relation, equation in Wapenaar and Fokkema (2006). The leading terms in this correlation will be of order α^2 , they are

$$\tilde{C}_{B,A}^3(\omega) = \frac{2c}{i\omega} \sum_{i=1}^A \quad (5.1)$$

$$G_0(\mathbf{x}_B, \mathbf{x}_s, \omega) G_1^*(\mathbf{x}_X, \mathbf{x}_s, \omega) G_1(\mathbf{x}_X, \mathbf{x}_s, \omega) G_0^*(\mathbf{x}_A, \mathbf{x}_s, \omega) + \quad (5.1)$$

$$G_0(\mathbf{x}_B, \mathbf{x}_s, \omega) G_1^*(\mathbf{x}_X, \mathbf{x}_s, \omega) G_0(\mathbf{x}_X, \mathbf{x}_s, \omega) G_1^*(\mathbf{x}_A, \mathbf{x}_s, \omega) + \quad (5.2)$$

$$G_1(\mathbf{x}_B, \mathbf{x}_s, \omega) G_0^*(\mathbf{x}_X, \mathbf{x}_s, \omega) G_0(\mathbf{x}_X, \mathbf{x}_s, \omega) G_1^*(\mathbf{x}_A, \mathbf{x}_s, \omega) + \quad (5.3)$$

$$G_1(\mathbf{x}_B, \mathbf{x}_s, \omega) G_0^*(\mathbf{x}_X, \mathbf{x}_s, \omega) G_0(\mathbf{x}_X, \mathbf{x}_s, \omega) G_1^*(\mathbf{x}_A, \mathbf{x}_s, \omega) + \quad (5.4)$$

$$O(\alpha^3).$$

Each term can be visualized using ray paths emitting from the source to a station or ray paths from a station to the source (for complex conjugated Green's functions). Terms 5.1, 5.2, 5.3 and 5.4 are represented in Figures 2(a), 2(b), 2(c) and 2(d) respectively.

STATIONARY PHASE ANALYSIS

The phases of terms 5.1, 5.2, 5.3 and 5.4 change rapidly as a function of source position, \mathbf{x}_s , auxiliary station position \mathbf{x}_X ,

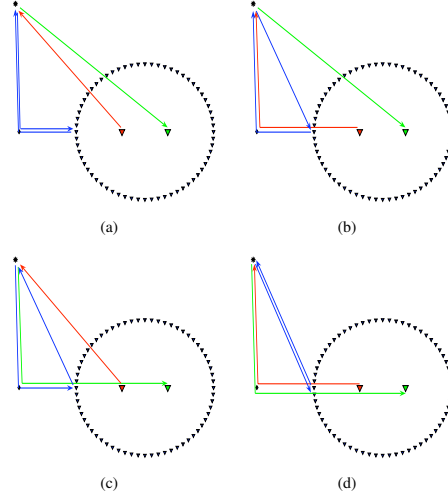


Figure 2: Visualization of the leading terms in $\tilde{C}_{A,a}^3$, Terms 5.1, 5.2, 5.3 and 5.4 in (a), (b), (c) and (d) respectively. Arrows from the source represent ray paths of Green's functions in the normal state; arrows to the source represent ray paths of Green's functions in the complex conjugated state.

the positions of the main stations \mathbf{x}_A and \mathbf{x}_B and scatterer position \mathbf{x}_c . (The phase of the scattered part of the Green's function, $G_1(\mathbf{x}, \mathbf{x}_s, \omega)$, changes rapidly as a function of the scatterer position \mathbf{x}_c .) The dominant contributions come from stationary phase positions of \mathbf{x}_A , \mathbf{x}_B , \mathbf{x}_X , \mathbf{x}_s and \mathbf{x}_c . The phases of terms 5.1, 5.2, 5.3 and 5.4, Ω_1 , Ω_2 , Ω_3 and Ω_4 respectively, are found using the Green's function in homogeneous media;

$$G(\mathbf{x}, \mathbf{x}_s, \omega) = \frac{1}{4\pi|\mathbf{x} - \mathbf{x}_s|} \exp \left\{ -i\omega c^{-1} |\mathbf{x} - \mathbf{x}_s| \right\}, \quad (5)$$

giving

$$\Omega_1 = \omega c^{-1} [|\mathbf{x}_B - \mathbf{x}_s| - |\mathbf{x}_A - \mathbf{x}_s|], \quad (6)$$

$$\Omega_2 = \omega c^{-1} [|\mathbf{x}_B - \mathbf{x}_s| - 2|\mathbf{x}_c - \mathbf{x}_s| - \quad (7)$$

$$|\mathbf{x}_X - \mathbf{x}_c| - |\mathbf{x}_A - \mathbf{x}_c| + |\mathbf{x}_X - \mathbf{x}_s|], \quad (8)$$

$$\Omega_3 = \omega c^{-1} [|\mathbf{x}_B - \mathbf{x}_c| + 2|\mathbf{x}_c - \mathbf{x}_s| - \quad (8)$$

$$|\mathbf{x}_X - \mathbf{x}_s| - |\mathbf{x}_A - \mathbf{x}_s| + |\mathbf{x}_X - \mathbf{x}_c|], \quad (9)$$

$$\Omega_4 = \omega c^{-1} [|\mathbf{x}_B - \mathbf{x}_c| - |\mathbf{x}_A - \mathbf{x}_c|]. \quad (9)$$

Analyzing the above four phases with the stationary phase method, requiring of $\nabla_{\mathbf{x}_X} \Omega = 0$, $\nabla_{\mathbf{x}_s} \Omega = 0$ and $\nabla_{\mathbf{x}_c} \Omega = 0$, gives stationary alignments of \mathbf{x}_s , \mathbf{x}_X , \mathbf{x}_c , \mathbf{x}_A and \mathbf{x}_B .

Phase Ω_1 is stationary with respect to \mathbf{x}_X and \mathbf{x}_c , because $\nabla_{\mathbf{x}_X} \Omega_1 = 0$ and $\nabla_{\mathbf{x}_c} \Omega_1 = 0$. The remaining requirement is that $\nabla_{\mathbf{x}_s} |\mathbf{x}_B - \mathbf{x}_s| = \nabla_{\mathbf{x}_s} |\mathbf{x}_A - \mathbf{x}_s|$. When the stations and source are aligned as $\mathbf{x}_s \rightarrow \mathbf{x}_A \rightarrow \mathbf{x}_B$, the phase is stationary and has the value $\Omega_1 = \omega c_0^{-1} |\mathbf{x}_B - \mathbf{x}_A|$, equal to that of the Green's function between stations A and B (see equation 5). When they align as $\mathbf{x}_s \rightarrow \mathbf{x}_B \rightarrow \mathbf{x}_A$ the phase is stationary, and its value $\Omega_1 = -\omega c_0^{-1} |\mathbf{x}_B - \mathbf{x}_A|$ is equal to that of the complex conjugate of the Green's function between stations A and B.

Phase Ω_2 is stationary when the source, scatterer, auxiliary receivers and main stations all align. When these are aligned

Kinematics of C^3

as $\mathbf{x}_s \rightarrow \mathbf{x}_c \rightarrow \mathbf{x}_X \rightarrow \mathbf{x}_A \rightarrow \mathbf{x}_B$, then $|\mathbf{x}_X - \mathbf{x}_s| = |\mathbf{x}_X - \mathbf{x}_c| + |\mathbf{x}_c - \mathbf{x}_s|$, $|\mathbf{x}_c - \mathbf{x}_s| + |\mathbf{x}_A - \mathbf{x}_c| = |\mathbf{x}_A - \mathbf{x}_s|$ and the phase $\Omega_2 = \omega c_0^{-1} |\mathbf{x}_B - \mathbf{x}_A|$. When stations A and B are reversed, the phase $\Omega_2 = -\omega c_0^{-1} |\mathbf{x}_B - \mathbf{x}_A|$. When the source position or/and scatterer position is fixed, the phase is stationary under alternative alignments of the main stations and auxiliary stations and has a different value.

Phase Ω_3 is similar to phase Ω_2 except that stations A and B should be reversed in the analysis. Thus when the source, scatterer, auxiliary receivers and main stations are aligned as $\mathbf{x}_s \rightarrow \mathbf{x}_c \rightarrow \mathbf{x}_X \rightarrow \mathbf{x}_B \rightarrow \mathbf{x}_A$, then the phase is stationary and valued $\Omega_3 = \omega c_0^{-1} |\mathbf{x}_B - \mathbf{x}_A|$. When $\mathbf{x}_s \rightarrow \mathbf{x}_c \rightarrow \mathbf{x}_X \rightarrow \mathbf{x}_A \rightarrow \mathbf{x}_B$, then the phase is stationary and valued $\Omega_3 = -\omega c_0^{-1} |\mathbf{x}_B - \mathbf{x}_A|$.

Phase Ω_4 is stationary with respect to \mathbf{x}_X and \mathbf{x}_s , because $\nabla_{\mathbf{x}_X} \Omega_1 = 0$ and $\nabla_{\mathbf{x}_s} \Omega_1 = 0$. The remaining requirement is that $\nabla_{\mathbf{x}_c} |\mathbf{x}_B - \mathbf{x}_c| = \nabla_{\mathbf{x}_c} |\mathbf{x}_A - \mathbf{x}_c|$. When the stations and scatterer are aligned as $\mathbf{x}_c \rightarrow \mathbf{x}_A \rightarrow \mathbf{x}_B$ the phase is stationary and valued $\Omega_4 = \omega c_0^{-1} |\mathbf{x}_B - \mathbf{x}_A|$. When they aligned as $\mathbf{x}_c \rightarrow \mathbf{x}_B \rightarrow \mathbf{x}_A$ the phase is stationary and valued $\Omega_4 = -\omega c_0^{-1} |\mathbf{x}_B - \mathbf{x}_A|$.

All four leading terms in $\tilde{C}_{B,A}^3(\omega)$ have stationary phases, but for terms 5.1, 5.2 and 5.3 the alignments stations, scatterer and source position are no different from the requirements for conventional SI (Snieder, 2004). However the fourth term, 5.4, is the relevant term that includes the contribution from the scatterer as in Figure 1(b). This term has stationary contributions independent of source positions. Its dependency on scatterer position is analogous to the sensitivity of conventional SI to source position.

KINEMATICS OF C^3

The ability of C^3 to improve EGF quality is further complicated by the effects of muting the dominant term 3.1 from $C_{A,X}^2(t)$ and $C_{B,X}^2(t)$. We study a simple example with two main stations A and B, surrounded by a network of auxiliary stations, X, in the presence of one source, s , whose energy is scattered by one additional scatterer, q . We analyze the kinematics of the events in C^3 using correlation gathers in two sets of numerical experiments.

We compute $C_{A,X}^2(\omega)$ and $C_{B,X}^2(\omega)$ as functions of auxiliary station position angle ϕ . The absolute values of their time domain equivalents are shown in Figures 4(a), 4(b). Events 1, 2 and 3 correspond to terms 3.1, 3.2, 3.3. The black lines indicate the travel time between the main station and each auxiliary station. The dominant term will, independent of source position, always reside within this window. The term of order α^2 is omitted to remain consistent with Born modeling, which is of order α .

The correlations are muted within the black lines, and the C^3 is formed for each auxiliary station. The absolute value of $\tilde{C}_{B,A}^3(t)$ before summation over auxiliary station is shown in Figure 7(a). Compare with Figure 7(b), where terms 5.1, 5.2, 5.3 and 5.4 (labeled 1, 2, 3 and 4), are computed directly, assuming we could perfectly omit term 3.1 from $C_{A,X}^2(\omega)$ and $C_{B,X}^2(\omega)$.

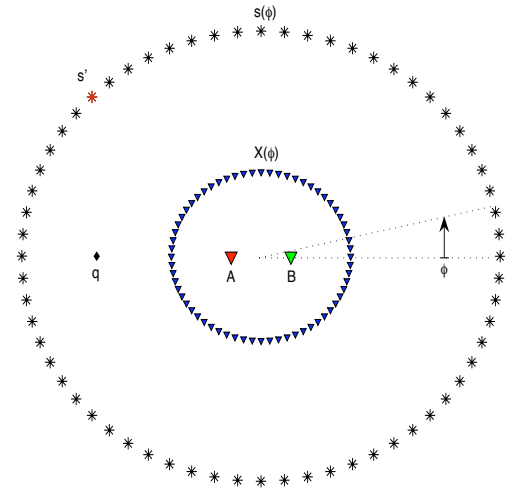


Figure 3: Geometry of numerical experiments. Main stations A, B and auxiliary stations X are represented by triangles, sources by asterisks, and the scatterer, q , by a diamond. A and B are 200 meters apart, q is located 450 meters from station A. Stations X and sources s are positioned as functions of ϕ at radii 300 and 800 meters respectively.

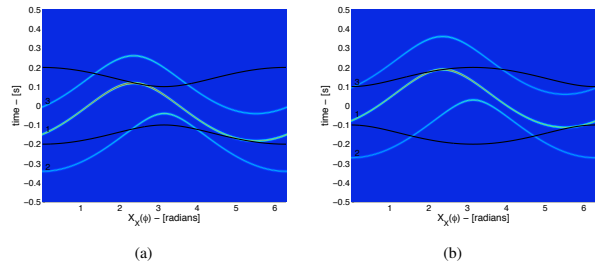


Figure 4: Gathers of $|C_{i,X}^2(t)|$ for each auxiliary station, $X(\phi)$, as a function of position angle ϕ , for $i = A$ in (a) and for $i = B$ in (b).

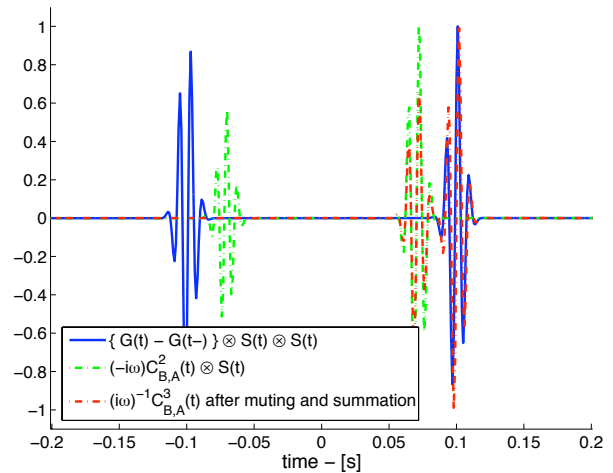


Figure 5: Comparison of the result of iterative SI (red), with conventional SI (green) and a direct modeled result (blue).

Kinematics of C^3

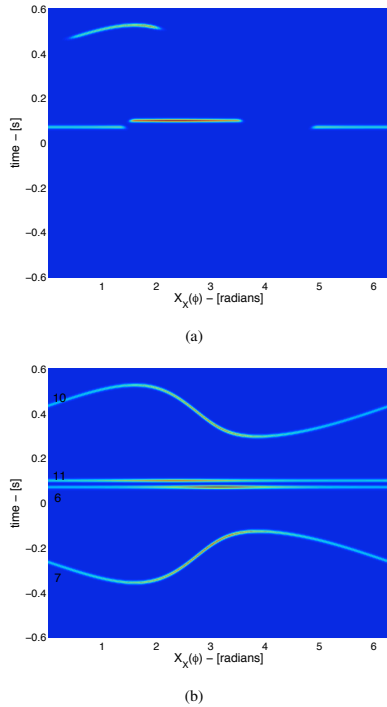


Figure 6: (a) Gather of $|\tilde{C}_{B,A}^3(t)|$ before stacking as a function of auxiliary station position angle ϕ . (b) gather showing time domain equivalents of 5.1, 5.2, 5.3 and 5.4 as a function of auxiliary station position angle ϕ .

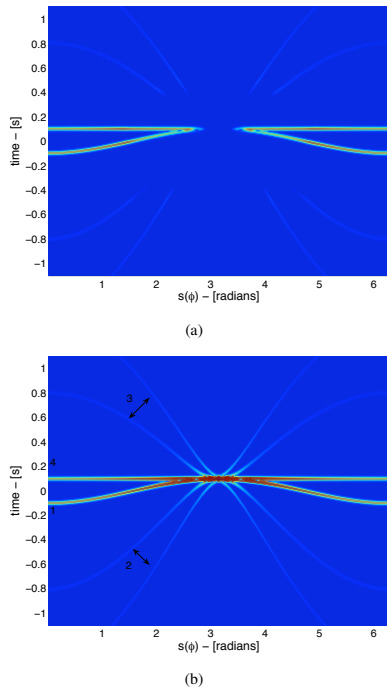


Figure 7: (a) Gather of $|\tilde{C}_{B,A}^3(t)|$ as a function of source position angle ϕ . (b) gather showing time-domain equivalents of 5.1, 5.2, 5.3 and 5.4 after summing over auxiliary station as a function of source position angle ϕ

The resulting signal, $\tilde{C}_{B,A}^3(t)$, is an EGF and is shown in Figure 5, compared to a directly computed Green's function convolved with the square of the autocorrelation of the source wavelet. It is also compared to an EGF by conventional SI ($C_{B,A}(t)$ convolved with the autocorrelation of the wavelet and multiplied by $-\frac{2i\omega}{c}$, Wapenaar and Fokkema (2006)). All signals are normalized to 1. It is clear that $\tilde{C}_{B,A}^3(\omega)$ exploits the scatterer to improve the quality of the EGF. Notice that $\tilde{C}_{B,A}^3(\omega)$ also contains an event at a spurious arrival time, similar to the spurious event in the EGF from conventional SI, as predicted by the stationary phase analysis of 5.1.

We study C^3 after summation over auxiliary stations. Figure 7(a) contains a gather of $\tilde{C}_{B,A}^3(t)$ for various source positions as a function of source position angle ϕ . Compare to Figure 7(b), where terms 5.1, 5.2, 5.3 and 5.4 (labeled 1, 2, 3 and 4), are computed directly. It is clear that for sources positioned at the stationary phase position, $\phi = \pi$, of terms 5.1, 5.2 and 5.3, the contribution from the scatterer becomes indistinguishable from the dominant term in $C_{A,X}^2(t)$ and $C_{B,X}^2(t)$. Notice how terms 5.1, 5.2 and 5.3 are non-stationary for most source positions except the source positions in the stationary phase regions of conventional ISI. For randomly positioned sources and outside stationary phase regions of conventional SI, the contributions of terms 5.1, 5.2, 5.3 combine destructively. The contribution of term 5.1 stands out and delivers an improved EGF.

CONCLUSIONS AND IMPLICATIONS FOR SEISMIC ACQUISITION GEOMETRIES

Iterative SI is a promising method to improve Green's function estimation by correlation of ambient seismic noise. We have studied the four leading terms in C^3 . One term is similar to the leading term in conventional SI and does not improve the EGF, but is sensitive to source position. Two terms are sensitive to the positions of the auxiliary stations and scatterer. Through averaging of C^3 over the auxiliary station network we become insensitive to these terms, as well as build the SNR. One leading term is completely insensitive to source location and auxiliary station position and provides illumination of the receivers through secondary scattering. The fourth term is sensitive to source location and provides the same illumination of the receivers as the leading term in conventional SI. Further study is needed to expand this method for specific station geometries in general inhomogeneous media. Iterative SI is a promising tool to improve EGFs from correlations and should be tested on 3D passive seismic field data. When receivers are located at the surface and the ambient seismic field consists of waves traveling predominantly in one direction along the surface, the EGF of surface waves between receivers perpendicular to that direction can be improved. When receivers are additionally located down-hole, the EGF of events traveling into the earth can potentially be improved.

ACKNOWLEDGMENTS

SdR and BB would like to thank the sponsors of the Stanford Exploration Project for their support.

EDITED REFERENCES

Note: This reference list is a copy-edited version of the reference list submitted by the author. Reference lists for the 2009 SEG Technical Program Expanded Abstracts have been copy edited so that references provided with the online metadata for each paper will achieve a high degree of linking to cited sources that appear on the Web.

REFERENCES

- Aki, K., 1957, Space and time spectra of stationary stochastic waves, with special reference to microtremors: *Bulletin of the Earthquake Research Institute*, **35**, 415–456.
- Artman, B., 2007, Passive seismic imaging: Ph.D. thesis, Stanford University.
- Claerbout, J. F., 1968, Synthesis of a layered medium from its acoustic transmission response: *Geophysics*, **33**, 264–269.
- de Ridder, S., and G. A. Prieto, 2008, Seismic interferometry and the spatial auto-correlation method on the regional coda of the non-proliferation experiment: *Eos Transactions, AGU, Abstracts*, S31A–1885.
- Garnier, J., and G. Papanocilaou, 2009, Passive sensor imaging using cross correlations of noisy signals in a scattering medium. Accepted for publication in *SIAM*.
- Lobkis, O. I. and R. L. Weaver, 2001, On the emergence of the greens function in the correlations of a diffuse field: *Journal of the Acoustical Society of America*, **110**, 3011–3017.
- Malcolm, A. E., J. A. Scales, and B. A. van Tiggelen, 2004, Retrieving the green function from diffuse, equipartitioned waves: *Physical Review E*, **70**, 015601–1–015601–4.
- Miyazawa, M., R. Snieder, and A. Venkataraman, 2008, Application of seismic interferometry to extract P- and S-wave propagation and observation of shear wave splitting from noise data at Cold lake, Canada: *Geophysics*, **73**, no. 4, D35–D40.
- Paul, A., M. Campillo, L. Margerin, E. Larose, and A. Derode, 2005, Empirical synthesis of time-asymmetrical Green functions from the correlation of coda waves: *Journal of Geophysical Research (Solid Earth)*, **110**, 8302.1–8302.13.
- Snieder, R., K. Wapenaar, and U. Wegler, 2007, Unified Green's function retrieval by cross-correlation; connection with energy principles: *Physical Review E*, **75**, 036103–1–036103–14.
- Snieder, R. K., 2004, Extracting the Green's function from the correlation of coda waves: A derivation based on stationary phase: *Physical Review E*, **69**, 046610–1–046620–8.
- Stehly, L., M. Campillo, B. Froment, and R. L. Weaver, 2008, Reconstructing Green's function by correlation of the coda of the correlation (c3) of ambient seismic noise: *Journal of Geophysical Research*, **113**, B11306.
- Stork, C. and S. Cole, 2007, Fixing the nonuniform directionality of seismic daylight interferometry may be crucial to its success: 77th Annual International Meeting, SEG, Expanded Abstracts, 2713–2717.
- Wapenaar, K., 2004, Retrieving the elastodynamic Green's function of an arbitrary inhomogeneous medium by cross correlation: *Physical Review Letters*, **93**, 254301–1–254301–4.
- Wapenaar, K., D. Draganov, and J. Robertsson, 2008a, Seismic interferometry: History and present status: *Geophysics Reprint Series No. 26*, SEG.
- Wapenaar, K., and J. Fokkema, 2006, Green's function representations for seismic interferometry: *Geophysics*, **71**, no. 4, SI33–SI46.
- Wapenaar, K., J. van der Neut, and E. Ruigrok, 2008b, Passive seismic interferometry by multidimensional deconvolution: *Geophysics*, **73**, no. 6, A51–A56.